Biochimica et Biophysica Acta 1798 (2010) 1301–1308

Contents lists available at ScienceDirect

Biochimica et Biophysica Acta

journal homepage: www.elsevier.com/locate/bbamem

Multiphoton excitation fluorescence microscopy in planar membrane systems

Jonathan Brewer, Jorge Bernardino de la Serna, Kerstin Wagner, Luis A. Bagatolli *

Membrane Biophysics and Biophotonics group/MEMPHYS, Center for Biomembrane Physics, Department of Biochemistry and Molecular Biology, University of Southern Denmark, Odense, Denmark

ARTICLE INFO

Article history:
Received 28 December 2009
Received in revised form 18 February 2010
Accepted 18 February 2010
Available online 10 March 2010

Keywords:
Langmuir films
LAURDAN
Two-photon excitation microscopy
Planar supported membranes

ABSTRACT

The feasibility of applying multiphoton excitation fluorescence microscopy-related techniques in planar membrane systems, such as lipid monolayers at the air–water interface (named Langmuir films), is presented and discussed in this paper. The non-linear fluorescence microscopy approach, allows obtaining spatially and temporally resolved information by exploiting the fluorescent properties of particular fluorescence probes. For instance, the use of environmental sensitive probes, such as LAURDAN, allows performing measurements using the LAURDAN generalized polarization function that in turn is sensitive to the local lipid packing in the membrane. The fact that LAURDAN exhibit homogeneous distribution in monolayers, particularly in systems displaying domain coexistence, overcomes a general problem observed when "classical" fluorescence probes are used to label Langmuir films, i.e. the inability to obtain simultaneous information from the two coexisting membrane regions. Also, the well described photoselection effect caused by excitation light on LAURDAN allows: (i) to qualitative infer tilting information of the monolayer when liquid condensed phases are present and (ii) to provide high contrast to visualize 3D membranous structures at the film's collapse pressure. In the last case, computation of the LAURDAN GP function provides information about lipid packing in these 3D structures. Additionally, LAURDAN GP values upon compression in monolayers were compared with those obtained in compositionally similar planar bilayer systems. At similar GP values we found, for both DOPC and DPPC, a correspondence between the molecular areas reported in monolayers and bilayers. This correspondence occurs when the lateral pressure of the monolayer is 26 ± 2 mN/m and 28 ± 3 mN/m for DOPC and DPPC, respectively.

1. Introduction

Lipid monolayers have a broad application in basic sciences (e.g. chemistry, biology, physical-chemistry, polymer science to mention a few). Even though this model represent "half of a bilayer" (one molecule thick), it is still extensively used to mimic basic molecular and supramolecular interactions among different types of lipids and proteins in membranes [1]. Examples of studies reported in monolayer systems at the air–water interface are (just to mention a few): (i) lateral structure of compositionally different lipid films [1–4], (ii) penetration studies of proteins, peptides or other drugs (anesthetics for example) into a monolayer [5–7], (iii) stability of peptide or protein monolayers [8,9], and (iv) enzymatic action of lipases [10–12]. Studies including rheological, topological, electrical and mechanical properties of monomolecular films are also accessible using Langmuir films [1,13,14]. For instance, studies of surface pressure and interfacial electrical potential as a function of average cross-sectional molecular area in Langmuir films provide insights into many interesting membrane-related parameters. Examples are lipid hydrocarbon chain ordering, lateral compressibility/elasticity, and dipole effects under various conditions including those that approximate one leaflet of a bilayer [1,13].

Importantly, Langmuir films have a concrete connection with relevant structures existing in biological systems. For example, it is well known that a proteo-lipid surfactant material exists in our body, e.g. in the respiratory airways, having important physiologically relevant functions [15]. Surfactant material is for example highly important during the breathing cycles in order to avoid lung collapse (by changing the surface tension in the surface of the alveoli) [15]. The organization of lung surfactant at the air–tissue interface has been modelled using monolayers (either Langmuir films or supported monolayers) composed of particular lipid mixtures (with or without proteins), surfactant lipid extracts and native surfactant material from different sources [16–21]. In most of the cases, the role of different components on the physical properties of the monolayer is evaluated under controlled environmental conditions [22,23].

At present, there is an array of different experimental techniques that can be used in order to study planar membrane model systems. Specifically, for Langmuir films the most classic measurements are the surface pressure (π), vs. molecular area isotherms and the surface potential-area isotherms [24]. However, additional structural information

* Corresponding author. Membrane Biophysics and Biophotonics group/MEMPHYS, Center for Biomembrane Physics, Department of Biochemistry and Molecular Biology, University of Southern Denmark, Campusvej 55, DK-5230 Odense M, Denmark.
E-mail address: bagatolli@memphys.sdu.dk (L.A. Bagatolli).

0005-2736/$ – see front matter © 2010 Elsevier B.V. All rights reserved.
doi:10.1016/j.bbamem.2010.02.024

can be obtained using spectroscopic techniques such as Brewster angle and fluorescence microscopy, UV-Vis, IR, Raman, Second harmonic generation, X-ray diffraction and reflectivity [25,26]. These applications can be classified in two types: (i) those that measure main properties of the whole monomolecular film and (ii) those that provide a spatial distribution of a measurable property of the monolayer in an image, such as those measured in microscopy-based techniques. For example, different fluorescence microscopy experiments can provide the spatial correlation of several interesting parameters, such as rotation of molecules, extent of hydration, polarity, local pH, and lateral diffusion. Applications of these aforementioned fluorescence microscopy approaches have become popular in the last 10 years using lipid bilayer systems; particularly giant unilamelar vesicles [27–29].

The first applications of fluorescence microscopy on Langmuir films were reported in the 1980s [3,30]. This very popular and frequently used experimental approach is based in the acquisition of images reflecting the distribution of a fluorescent probe in the monolayer film upon compression. Although, as we mentioned above, fluorescent microscopy techniques offer the possibility of measuring of a variety of fluorescent parameters in the target system, this type of approach has not been fully exploited in Langmuir films except for a few exceptions [31,32].

This present report introduces and discusses for first time multiphoton excitation fluorescence microscopy applications in Langmuir films using the fluorescence probe LAURDAN. Additionally we describe some technical details about our systems, where a Langmuir trough has been incorporate on a custom built multiphoton excitation fluorescence microscopy.

2. Materials and methods

1,2-dipalmitoyl-*sn*-glycero-3-phosphocholine (DPPC) and 1,2-dioleoyl-*sn*-glycero-3-phosphocholine (DOPC) were purchased from Avanti Polar Lipids and used without further purification. 6-dodecanoyl-2-dimethylamino naphthalene (LAURDAN) was obtained from Invitrogen (Denmark).

2.1. Preparation of Langmuir films

A solution of 1 mg/ml DPPC (or DOPC) dissolved in a chloroform mixed with 2 mol% of LAURDAN was prepared. 20 µl of the solution was carefully added to the air/water interface and the solvent was allowed to evaporate over 10 min. The trough has a maximum area of 312 cm^2 and a minimum area of 54 cm^2 and uses Teflon-coated ribbons as the barriers. The ribbons are moved so as to compress as a symmetrical double barrier. The pressure was measured using the Wilhelmy plate technique. We estimate the error between different isotherms to be on the order of ± 1 mN/m. The monolayer was compressed at a speed of 50 cm^2/min to the desired surface pressure, which was kept constant during the laser scanning experiments. The experiments were carried out on a MilliQ-water subphase at room temperature (room temperature, 21 °C). The data sets for the GP functions were based on 2 or 3 independent measurements of different monolayers of DOPC or DPPC, respectively.

2.2. Preparation of supported lipid membranes by spincoating

The preparation of supported membranes by hydration of spin-coated lipid films has been described previously [33,34]. To prepare the dry spin-coated lipid film on mica, we used a stock solution of 10 mM lipid containing 0.5 mol % LAURDAN in hexane/methanol (97:3 volume ratio). 30 µL of this lipid stock solution was then applied to freshly cleaved mica and immediately thereafter spun on a Chemat Technology, KW-4A spin-coater at 3000 rpm for 40 s. The sample was then placed under vacuum for 10–15 h to ensure complete removal of the organic solvents. The dry spincoated film was subsequently hydrated by immersing the sample in either pure water or phosphate buffer (10 mM phosphate, 128 mM NaCl, pH = 7) followed by heating to 55 °C for 1 h. The sample was then placed on the fluorescence microscope and flushed with 55 °C buffer/water using a pipette adjusted to 500 µL in order to remove excess lipid from the support. After the washing procedure, the liquid volume was gently exchanged 5–10 times to remove membranes in solution. Measurements of LAURDAN GP function in these membranes were performed using the same setup indicated in the next section. The GP experiments have been carried out twice and multiple images (up to 15) were collected from each individual samples. No substantial difference in the GP value was found between the samples made in pure water or those made in buffer.

2.3. LAURDAN GP function

The LAURDAN GP denotes the position of the probe's emission spectrum [35]. The fluorescence emission properties of LAURDAN are sensitive to the water dipolar relaxation process that occurs in the probe's environment. The energy of the excited singlet state progressively decreases when the extent of dipolar relaxation process is augmented. The extent of water dipolar relaxation observed in highly packed membrane regions (as the solid-ordered phase in bilayers) is very low compared to what it is observed in less packed regions (as the liquid-disordered phase in bilayers). For example when a solid-ordered/liquid-disordered phase transition occurs in the membrane, a prominent red shift in the fluorescence emission spectrum of the probe is observed (from blue to green; almost 50 nm shift) [35]. The GP function was defined analogously to the fluorescence polarization function as:

$$GP = \frac{I_B - I_R}{I_B + I_R} \quad (1)$$

where I_B and I_R correspond to the intensities at the blue and red edges of the emission spectrum (440 and 490 nm) using a given excitation wavelength [35–37]. In lipid bilayers high LAURDAN GP values (0.5–0.6) correspond to laterally ordered phases (e.g. solid-ordered or gel) whereas low LAURDAN GP values (below 0.1) correspond to liquid-disordered phases [35]. Coexistence of liquid-ordered and liquid-disordered lipid phases in bilayer systems have been characterized using LAURDAN GP images [38,39].

2.4. LAURDAN GP measurements

For LAURDAN GP measurements the fluorescence signals were collected in two different channels using bandpass filters of 438 ± 12 nm and 494 ± 10 nm. The fluorescence emission light was split between two PMTs (Hamamatsu H7422P-40) by a dichromatic Mirror splitting at 475 nm. The microscope is controlled by Globals for Images SimFCS. This software is developed by the Laboratory for Fluorescence Dynamics, University of California at Irvine, USA. It is important to notice that the GP values obtained from the GP images strongly depend on instrumental factors such as filter settings and gain of the PMTs used in the microscope. Therefore, the calculated GP images must be calibrated with a correcting factor G. As the GP function is based on the relative intensity of the blue and the green channel it is necessary to calibrate the relative intensity of the two channels to obtain an absolute measurement of the GP. Therefore the GP equation utilized to calculate the GP images contains a factor G (similar to the classical polarization equation), used in this case to calibrate the relative intensity of the two channels:

$$GP = \frac{I_B - (G \times I_R)}{I_B + (G \times I_R)} \quad (2)$$

In Eq. (2) the GP should be equal to that from a reference solution with a defined GP. The measurement of the factor G is performed by

acquiring images of a LAURDAN reference solution with a known GP in the microscope using the same instrumental conditions as in the membrane experiments [34]. The GP value from the microscope is then corrected using the G factor so that it matches the reference value measured on the fluorometer (this is done from the SimFCS software). The G factor can be calculated from the above equation as:

$$G = \frac{I_B(1-GP_c)}{I_R(GP_c + 1)} \quad (3)$$

where GP_c is the GP value from the reference solution measured in the fluorometer. The obtained G factor is then used to calibrate the GP values from images of the monolayer. In our experiments we used a 160 μM LAURDAN solution in DMSO as a reference (GP = 0.006 at room temperature). The LAURDAN GP value of the reference solution was measured in a fluorometer (ISS, Champaign, IL, USA) at the emission wavelengths defined for Eq. (1), i.e. the excitation wavelength was 374 nm and the emission wavelengths 440 nm and 490 nm. The associated error of the GP measurements from the Langmuir films is ±0.03.

2.5. LAURDAN photoselection effect

The photoselection effect arises from the fact that only those fluorophores which have electronic (absorption) transition moments aligned parallel or nearly so to the plane of polarization of the excitation light are excited, i.e. the excitation efficiency is proportional to the fourth power of the cosine (for two photon excitation, cosine square for one photon excitation) of the angle between the electronic transition moment of the probe and the polarization plane of the excitation light [27,34]. In our particular monolayer setup, we expect to observe differences in the fluorescence intensity between ordered and disordered regions, but also to be sensitive to changes in the orientation of the membrane, particularly when condensed phases are present or when the monolayer is at the collapse point (similar to the effects previously described between the equatorial and polar regions of GUVs, [27,40]). This phenomenon is illustrated in Fig. 1A.

In order to perform comparative LAURDAN GP experiments between monolayer and bilayers we choose planar supported bilayers as a reference, because of the similar planar geometry between these two systems. Studies exploiting the LAURDAN GP function have been recently reported in planar membrane systems in order to explore the texture of gel domains in bilayer model systems [34].

2.6. Custom built Fluorescence microscope for monolayers

The measurements reported in this paper were made on a custom built multiphoton excitation microscope. This setup is specially constructed on an Olympus IX70 microscope. The objective used in the experiments was a 60× water immersion objective with an NA of 1.2. The excitation light source was a femtosecond Ti:Sa laser (Broadband Mai Tai XF-W2S with 10 W Millennia pump laser, tunable excitation range 710–980 nm, Spectra Physics, Mountain View, CA) and the excitation wavelength was 780 nm. The excitation light was circularly polarized to avoid photoselection effect in the plane of the monolayer. This allows to selectively observe photoselection along the *z* direction.

A special designed Langmuir Blodgett trough built by NIMA (Coventry, UK) was mounted on top of the microscope. The trough has a maximum area of 312 cm^2 and a minimum area of 54 cm^2 and uses Teflon-coated ribbons as the barriers. The trough features a window in the center of the bottom of the trough, designed to enable imaging of a monolayer on the water surface with the 60× water objective from below the trough (see Figs. 1B and 2). The microscope and trough were mounted on an actively stabilized optical table from Newport to minimize vibration. To help stabilize the thin water film on the glass window, the glass was made hydrophilic by using a plasma cleaner (Harrick Plasma, Ithaca, NY) for 15 min before use.

3. Results and discussion

To investigate the behavior of LAURDAN in lipid monolayers, we performed two photon excitation fluorescence microscopy experiments on Langmuir films composed of either pure DPPC or DOPC. As shown in Fig. 3, the LAURDAN distribution in the plane of the monolayer is homogeneous in these two compositionally different monolayer systems upon compression. This phenomenon is also observed in the case of the DPPC film, where coexistence of distinct lipid phases is present at particular lateral pressures (Fig. 3B). The homogenous distribution of LAURDAN observed in our monolayer experiments is in agreement with that previously reported for LAURDAN in giant unilamellar vesicles (GUVs) composed of binary and ternary mixtures showing coexistence of phases [39,41–44]. The obtained results show an interesting advantage of the LAURDAN

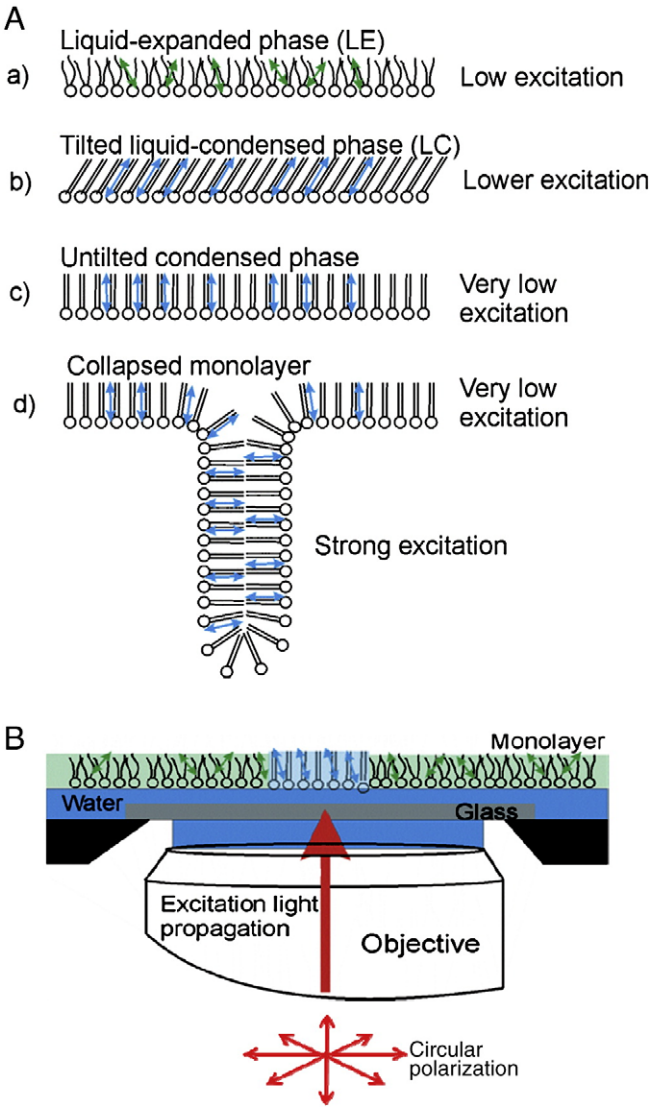

Fig. 1. (A) Sketch displaying the orientation of the LAURDAN transition moment in monolayers displaying different phases (a-d). (B) Sketch showing the coupling between the water immersion objective (located in our custom built microscope) and the Langmuir trough. The drawing shows a lipid monolayer at the air/water interface and includes the glass window (coverglass) located at the bottom of the trough in order to observed the monolayer. The blue and green arrows in the lipid monolayer represent the transition moments of LAURDAN in a liquid-condensed and liquid-expanded phases, respectively. The sketch is not drawn to scale.

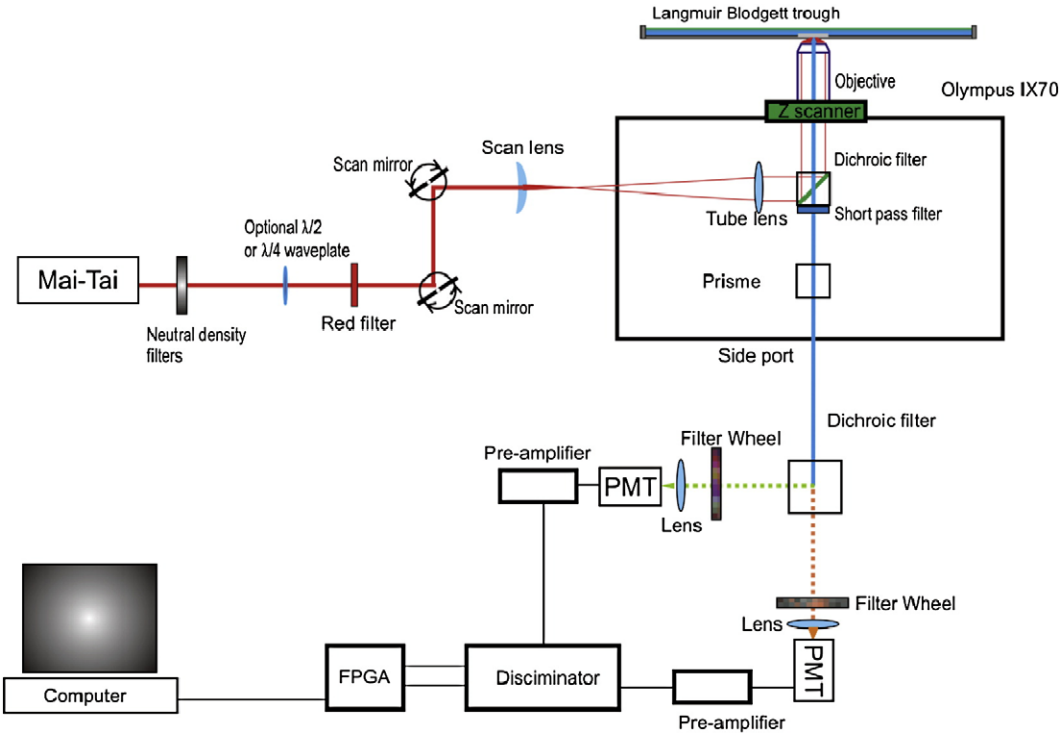

Fig. 2. Sketch showing our complete experimental setup, consisting in a custom built multiphoton excitation fluorescence microscope and a Langmuir trough. The microscope detection unit was operated in photon counting mode.

probe over classical fluorescent probes used in monolayer experiments, particularly when distinct membrane domains are observed in the lipid film. Most of the fluorescent probes used in monolayer experiments (e.g. NBD-PC, Bodipy-PC) display preferential partition to one domain type in the lipid film. This last situation precludes obtaining simultaneous information from different coexisting membrane regions, for example by exploiting the probe's fluorescent parameters (such as maximum emission wavelength, polarization, fluorescence lifetime). Certainly the use of LAURDAN overcomes this limitation. When phase coexistence is present in the lipid film, the use of a single probe (LAURDAN) allows obtaining spatially resolved information about local lipid packing in different regions of the monolayer (GP function images).

3.1. Gas and liquid-expanded phase

From the LAURDAN GP data presented in Fig. 3A and B it is clear that the extent of water dipolar relaxation phenomenon experienced by the probe in the Langmuir film is depending on the particular phase present in the monolayer. This phenomenon is very well reflected by the very low GP value measured in the region of gas/liquid-expanded phase coexistence (below −0.5), both in DOPC and DPPC monolayers. As shown in Fig. 4A and B, the LAURDAN GP function gradually increases upon compression reaching a value of −0.3 at ~23 mN/m for DOPC, or at ~12 mN/m for DPPC (notice that in this last case we are referring to the GP measured in the more fluid regions of the DPPC monolayers, Fig. 3B). From the presented experimental data we can conclude that LAURDAN is sensitive to the physical changes exerted in the monolayer upon compression. Particularly, these results show a clear response of the probe when a liquid-expanded phase is formed at expense of a gas phase in the monolayer.

The lowest LAURDAN GP value reported in bilayer systems (around −0.25) is obtained when these membranes are in a liquid-disordered phase (L_α) [27]. Following the interpretation of the LAURDAN GP function in bilayer systems, we can conclude that LAURDAN experiences a highly hydrated environment in the gas phase, with a subsequent decrease in the extent of water relaxation phenomenon when the monolayer displays a liquid-expanded phase. Interestingly, this is the first time where such a range of low LAURDAN GP values (−0.6 to −0.3) is reported for a lipid membrane, indicating one more time the strong sensitivity of the LAURDAN GP function to the physical state of the host membrane [42,45].

3.2. Liquid-expanded/liquid-condensed phase coexistence

In these experiments we used the very well-characterized DPPC films at the air–water interface. DPPC isotherms at 20 °C show a region corresponding with coexistence of liquid-expanded and liquid-condensed phases [46,47]. Therefore this system is very suitable to explore the response of LAURDAN in monolayers displaying phase coexistence.

Fig. 3. (A) Surface pressure/area isotherm for the compression of a DOPC monolayer at room temperature (21 °C) (left). Representative LAURDAN fluorescence intensity and GP images of a DOPC monolayer at different surface pressures (a–c) (right). The green and blue fluorescence intensity images have the same fluorescence intensity scale and are represented in false colors. The pressures indicated in the images are a) 1.8 mN/m (average GP value is −0.53, b) 25.5 mN/m (average GP value is −0.26), c) 37.5 mN/m (average GP value is −0.10). The scale bar (for all microscopy images presented in the figure) is 10 μm. (B) Surface pressure/area isotherm for the compression of a DPPC monolayer at room temperature (21 °C) (left). Representative LAURDAN fluorescence intensity (blue and green channels) and GP images of a DPPC monolayer at different surface pressures (a–e) (right). The blue and green intensity images have the same fluorescence intensity scales and are represented in false colors. The pressures indicated in the images are: (a) 3.8 mN/m (average GP value is −0.58), (b) and (c) 8.8 mN/m (average GP value in liquid-expanded and liquid-condensed are −0.32 and 0.44, respectively), (d) 30 mN/m (average GP value is 0.55), (e) 70 mN/m (average GP value is 0.62). At the collapse pressure the gain of the detectors has been reduced to avoid saturation on the high fluorescence intensity areas, i.e. the collapsed structures. For such reason the GP values shown in (e), except those obtained in the collapse areas, are meaningless. For both A and B the experimental error on the measured GP values is ±0.03.

At pressures above 4 mN/m we observed distinct domains in the monolayer displaying high blue LAURDAN emission intensity. These domains were surrounded by areas displaying high green intensity emission (Fig. 3B). These high blue fluorescence intensity domains show bean/kidney and trilobal/spiral shapes similar to that previously reported as liquid condensed domains in DPPC films [47,48]. In

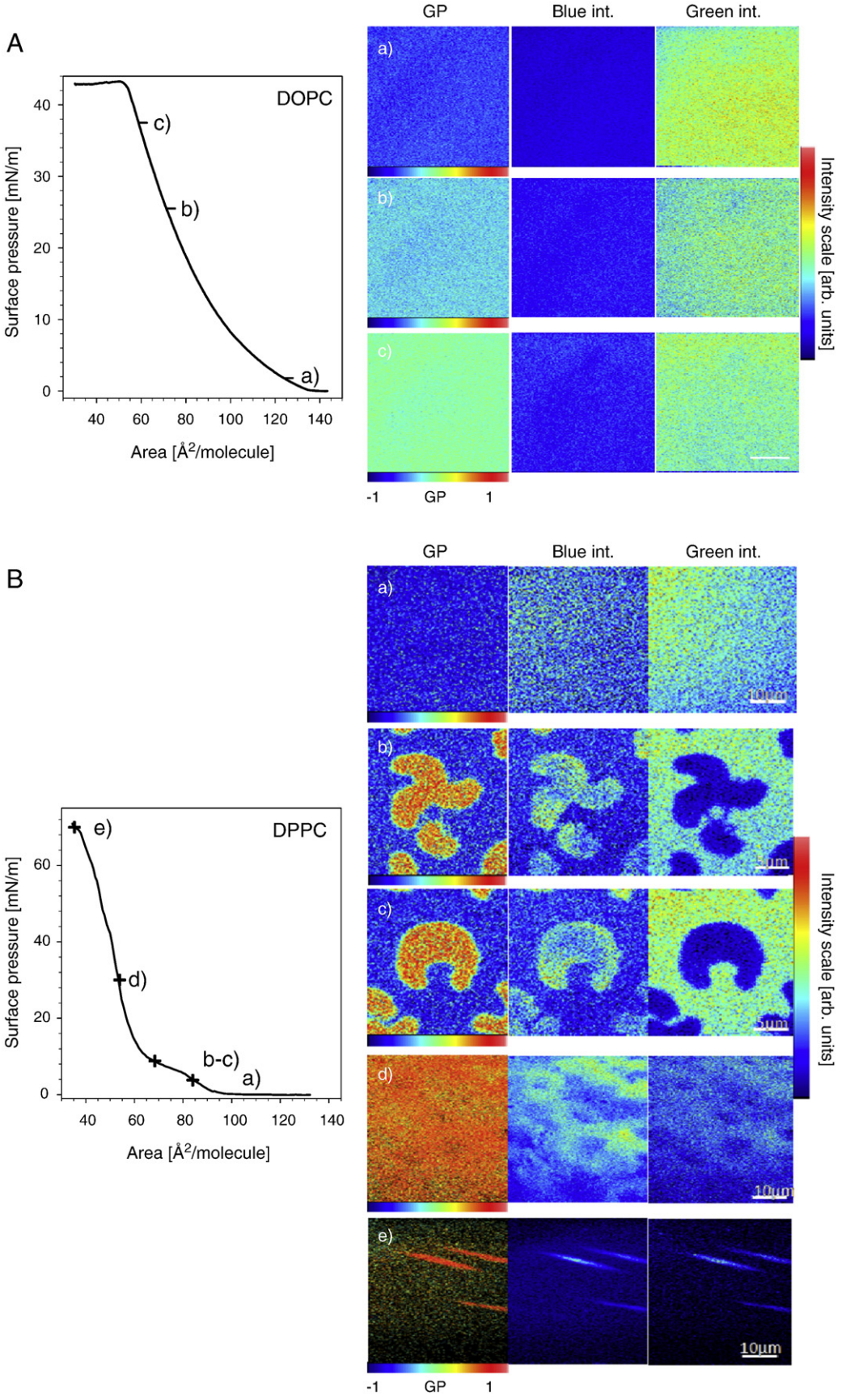

addition, these particular domains show higher GP values (low extent of water dipolar relaxation process/higher packing) with respect to that observed in the rest of the film (Fig. 3B). At this point we can conclude that the reported data correspond very well to the liquid-expanded/liquid-condensed coexistence region previously reported for DPPC monolayers. Between 12 and 15 mN/m, the high GP regions (liquid-condensed) starts to percolate, and above ~18 mN/m no distinguishable low GP (liquid-expanded) regions were observed in the film.

The LAURDAN GP values obtained in the liquid-condensed regions augment from approximately 0.22 to 0.55 as the pressure is raised from 4 to ~30 mN/m (Fig. 4B). This result indicates a progressive decrease in the extent of water relaxation process occurring in this phase caused by the reduction of the area per lipid upon compression (similar to our observations for both DOPC and DPPC in the liquid-expanded phase; cf. Fig. 4A and B). At surface pressures above 33 mN/m, the GP measured for the condensed phase of DPPC is constant at ~0.6. The upper end of the range of observed GP values is in line with that observed for solid ordered (gel) phases in lipid bilayers (Fig. 4B; [27]).

Up to 30 mN/m, a gradual decrease in the intensity of the overall LAURDAN fluorescence emission is observed. It has been reported that between 10 and 30 mN/m, the tilting of the DPPC chains with respect to the surface normal is reduced by 7° (from approximately 39° to 32° [49,50]). This decreased tilting affects the LAURDAN orientation and lead to an increase in the photoselection effect (cf. Fig. 1A). However, the lack of a drastic reduction in the overall LAURDAN intensity (as the one observed above 30 mN/m, cf. below) may be compensated by an increase in the probe density during reducing the area upon compression.

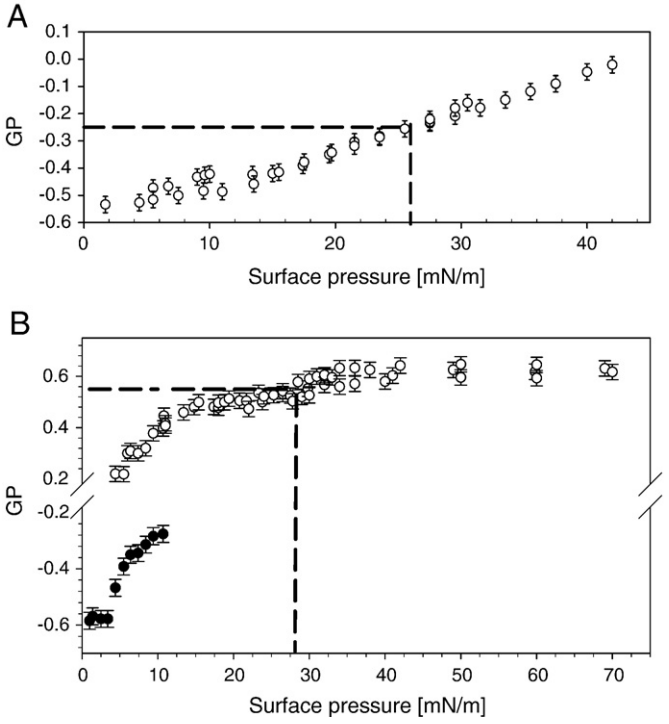

Fig. 4. (A) LAURDAN GP values from a DOPC monolayer at different pressures (open circles). The dashed line shows the intersection between the progression of the monolayer GP values and the GP value measured in a DOPC supported planar bilayer membrane (−0.25 ± 0.03). The intersection was found at 26 ± 2 mN/m. (B) LAURDAN GP values from a DPPC monolayer at different pressures (circles). The filled symbol represents measurements on gas and liquid-expanded phases, while the open symbol corresponds to liquid condensed phases. The dashed line shows the intersection between the GP progression obtained for the liquid condensed phase and the corresponding GP (0.55 ± 0.03) value measured in a DPPC supported planar bilayer membrane. The intersection was found at 28 ± 3 mN/m. For both A and B the experimental error on the measured GP values is ± 0.03.

Based on previous information reported for LAURDAN in bilayer systems displaying gel/fluid phase coexistence [41–43], the situation observed in the DPPC monolayers corresponds very well with a coexistence of two different regions showing high and low lipid packing. As we mentioned above, this information is in line with coexisting liquid expanded and liquid condensed phases reported for DPPC films [46–48]. This last result illustrates the capability of LAURDAN to simultaneously map the physical properties of coexisting phases not only in lipid bilayers but in lipid films at the air–water interface.

3.3. Lipid tilting in liquid-condensed regions

It is interesting to note that at 30 mN/m, although the GP function is (nearly) homogeneous, the intensity images obtained in the green and blue channels are not. In fact, the nature of the aforementioned fluorescence intensity patterns is different to those observed when coexistence of liquid-expanded/liquid condensed phases is present in the monolayer (where a strong correspondence between high GP/high blue fluorescence intensity and low GP/high green fluorescence intensity is observed; see Fig. 3B and compare images b and c with image d). The fluorescence intensity images obtained at 30 mN/m (Fig. 3B d) shows that the high intensity areas co-localize in both green and blue channels. In order to explain this phenomenon we consider that at 30 mN/m: (i) the orientation of the probe in these two distinct fluorescence intensity regions is different (intensity differences are only due to the photoselection effect), and (ii) the extent of water dipolar relaxation process (reflected in the LAURDAN GP function) is becoming very similar between two distinct fluorescence intensity regions.

Above 30 mN/m, the overall fluorescence intensity emitted from LAURDAN dramatically decreases upon compression (compared Fig. 3B, d and e), i.e. the intensity in both channels drops more than 3 folds when the monolayer is compressed from 30 to 40 mN/m. In other words, there must be a continued change in the orientation of the probe's transition moment in the liquid-condensed film upon compression above 30 mN/m (see Fig. 1A). In fact, from 30 to 40 mN/m, the DPPC tilting is further reduced by 3 to 4° [49,50] affecting the LAURDAN orientation in the monolayer (and producing a large effect of photoselection). We believe that the effect of intensity loss due to the photoselection is much bigger and more critical than the potential augmentation of intensity due to a higher probe density upon compression. In fact, because of the highly reduced compressibility of the DPPC monolayer at high surface pressures, the LAURDAN density can hardly be further increased above 30 mN/m.

At this point this is a qualitative effect since we are not yet able to determine tilting angles using this approach. However, studies exploiting the LAURDAN fluorescence polarization simultaneously with the GP function have been recently reported in planar bilayer membranes composed of binary lipid mixtures to explore the gel domain's texture [34]. We believe that this combined experimental approach can be potentially utilized in monolayer experiments to explore tilting (and texture) effects on different lipid domains.

3.4. Collapse pressure

As mentioned above, the fluorescence emitted by LAURDAN in the DPPC films becomes weaker as the pressure is raised above 30 mN/m due to the photoselection effect. However, at ~70 mN/m we observed high fluorescence intensity lines in the plane of the images obtained in the monolayer (Fig. 3B, e). This phenomenon is again indicative of a dramatic change in the orientation of the probe with respect to the polarization plane of the excitation light (Fig. 1A, d). In other words, we believe that the probe's reorientation is caused by the collapse of

the monolayer towards the water phase. The GP value measured in these particular regions is ~0.55, a similar value obtained from gel-phase DPPC planar supported bilayers (see below). The last observation might suggest a correspondence between the collapsed structures and bilayers (notice that the GP measured in the plane of monolayer at 70 mN/m pressure is ~0.62, Fig. 4B).

3.5. Bilayer and monolayer correspondence

We decided to explore if the dependence of LAURDAN GP function in monolayers upon compression can be somehow connected with the values obtained in bilayers. To answer this question we decided to compare the LAURDAN GP values obtained in Langmuir films upon compression with those obtained in compositionally similar planar bilayer membranes since the geometry of both system is the same (i.e. planar). At similar GP values, we observed for both DOPC and DPPC, a correspondence between the measured molecular areas in the monolayer experiment and the reported molecular area in bilayers of similar compositions (Fig. 4A and B). For example, DOPC bilayers have the same GP value of -0.25 ± 0.03 as DOPC monolayers at 26 ± 2 mN/m (Fig. 4A). This value corresponds to an area per lipid molecule of ~71 Å^2 as seen in the compression isotherm (Fig. 3A). The obtained area is in line with the range of areas per lipid molecule reported for DOPC bilayers in the liquid disordered phase, i.e., from 70.1 to 72.6 Å^2 (values measured between 20 and 25 °C) [51,52]. For DPPC on the other hand, the equivalent GP value between monolayers at 28 ± 3 mN/m and bilayers is 0.55 ± 0.03 (Fig. 4B). This value corresponds to an area per lipid molecule of 54 Å^2 as seen in the compression isotherm (Fig. 3B). This area value is close (but slightly higher) than the values reported for DPPC bilayers displaying a gel phase (from 47.9 to 52.3 Å^2, values measured between 20 and 25 °C) [53].

It is striking that the LAURDAN GP's correspondence between DPPC monolayers and bilayers match with the 30 mN/m pressure regime found in monolayers. It is exactly this pressure regime where other structural parameters of DPPC monolayers concur most with those of DPPC bilayers [53]. For example, it was reported that at 30 mN/m, DPPC monolayers exhibit a 32° tilt of the lipid chains and an area per lipid molecule of 48 Å^2 as determined by X-ray measurements [49,50,54]. Fully hydrated bilayers at nearly the same temperature also show a lipid chain tilt of 32° and a molecular area of 47.2 Å [55]. The parallelism of these structural parameters (around 30 mN/m) in bilayers and monolayers shows that the hydration state of both membrane systems is comparable. The correspondence of the GP value strengthens the point that lipid bilayers and monolayers in the pressure regime of 30 mN/m possess equivalent structures [52]. However, especially DOPC shows this equivalence of monolayer and bilayer structures at a slightly lower surface pressure of the monolayer than the previously reported 30 to 35 mN/m range [56]. Hence, systematic studies with compositionally different system are required to further explore this monolayer/bilayer equivalence. This step is necessary to generalize our hypothesis and conclusions about the bilayer–monolayer correspondence.

4. Concluding remarks

We demonstrate that the fluorescence probe LAURDAN shows homogeneous partition in lipid films at the air–water interface, even in cases where domain coexistence is observed. By exploiting the sensitivity of this probe to lipid packing we can obtain spatially resolved information using the LAURDAN GP function in different regions of the lipid film, overcoming a problem generally observed from "classical" fluorescence probes used in monolayers studies (e.g. NBD-PC, Bodipy-PC), i.e. they label only one particular region of the film when lipid phase coexistence is observed. As it was argued in bilayer systems [27], the partition of these "classical" fluorescence probes can be dependent on the composition of the lipid domains making it risky to infer the local phase state of the lipid domain from the fluorescence images. This last disadvantage is clearly solved by the use of LAURDAN. Also, while the GP function provides clear differences among gas, liquid-expanded and liquid-condensed phases, the photoselection effect on LAURDAN gives extra capabilities to discriminate different tilting on condensed phases and identified membrane structures at the collapse point. Last but not least, we demonstrated that a connection between monolayers and bilayers can be performed exploiting the LAURDAN GP function in both systems. This approach can be further extended by performing measurements of lifetime (FLIM), polarization (anisotropy imaging) and/or diffusion (see Ref. [32] describing FCS experiments in monolayers) of the probe in the films using microscopy based techniques.

Acknowledgments

This work was supported by funds from Forskningsrådet for Natur og Univers (FNU, Denmark) and the Danish National Research Foundation (which supports MEMPHYS-Center for Biomembrane Physics).

References

[1] R.E. Brown, H.L. Brockman, Using monomolecular films to characterize lipid lateral interactions, Methods Mol. Biol. (Clifton, NJ) 398 (2007) 41–58.
[2] B. Maggio, The surface behavior of glycosphingolipids in biomembranes: a new frontier of molecular ecology, Prog. Biophys. Mol. Biol. 62 (1994) 55–117.
[3] H.M. McConnell, L.K. Tamm, R.M. Weis, Periodic structures in lipid monolayer phase transitions, Proc. Natl. Acad. Sci. U. S. A. 81 (1984) 3249–3253.
[4] R.G. Oliveira, B. Maggio, Compositional domain immiscibility in whole myelin monolayers at the air–water interface and Langmuir-Blodgett films, Biochim. Biophys. Acta 1561 (2002) 238–250.
[5] G.D. Fidelio, B.M. Austen, D. Chapman, J.A. Lucy, Properties of signal-sequence peptides at an air–water interface, Biochem. J. 238 (1986) 301–304.
[6] R. Maget-Dana, The monolayer technique: a potent tool for studying the interfacial properties of antimicrobial and membrane-lytic peptides and their interactions with lipid membranes, Biochim. Biophys. Acta 1462 (1999) 109–140.
[7] S. Choi, S. Oh, J. Lee, Effects of lidocaine-HCl salt and benzocaine on the expansion of lipid monolayers employed as bio-mimicking cell membrane, Colloids Surf. 20 (2001) 239–244.
[8] E.E. Ambroggio, F. Separovic, J. Bowie, G.D. Fidelio, Surface behaviour and peptide-lipid interactions of the antibiotic peptides, Maculatin and Citropin, Biochim. Biophys. Acta 1664 (2004) 31–37.
[9] I.Y. Churbanova, A. Tronin, J. Strzalka, T. Gog, I. Kuzmenko, J.S. Johansson, et al., Monolayers of a model anesthetic-binding membrane protein: formation, characterization, and halothane-binding affinity, Biophys. J. 90 (2006) 3255–3266.
[10] I.D. Bianco, G.D. Fidelio, R.K. Yu, B. Maggio, Degradation of dilauroylphosphatidylcholine by phospholipase A2 in monolayers containing glycosphingolipids, Biochemistry 30 (1991) 1709–1714.
[11] G. Pieroni, Y. Gargouri, L. Sarda, R. Verger, Interactions of lipases with lipid monolayers. Facts and questions, Adv. Colloid Interface Sci. 32 (1990) 341–378.
[12] K. Wagner, G. Brezesinski, Phospholipase D activity is regulated by product segregation and the structure formation of phosphatidic acid within model membranes, Biophys. J. 93 (2007) 2373–2383.
[13] G. Leneweit, M. Vranceanu, K. Winkler, H. Nirschl, Surface rheology and phase transitions of monolayers of phospholipid/cholesterol mixtures, Biophys. J. 94 (10) (2008) 3924–3934.
[14] L.R. Arriaga, I. Lopez-Montero, R. Rodriguez-Garcia, F. Monroy, Nonlinear dilational mechanics of Langmuir lipid monolayers: a lateral diffusion mechanism, Phys. Rev. E (2008) 77.
[15] R. Notter, Lung surfactants: basic science and clinical applications (lung biology in health and disease), Marcel Dekker Inc, New York, 2000.
[16] G.W. Paul, R.J. Hassett, O.K. Reiss, Formation of lung surfactant films from intact lamellar bodies, Proc. Natl. Acad. Sci. U. S. A. 74 (1977) 3617–3620.
[17] K. Nag, J. Perez-Gil, M.L. Ruano, L.A. Worthman, J. Stewart, C. Casals, et al., Phase transitions in films of lung surfactant at the air–water interface, Biophys. J. 74 (1998) 2983–2995.
[18] B. Piknova, V. Schram, S.B. Hall, Pulmonary surfactant: phase behavior and function, Curr. Opin. Struct. Biol. 12 (2002) 487–494.
[19] W. Yan, S.C. Biswas, T.G. Laderas, S.B. Hall, The melting of pulmonary surfactant monolayers, J. Appl. Physiol. 102 (2007) 1739–1745.
[20] L. Wang, A. Cruz, C.R. Flach, J. Perez-Gil, R. Mendelsohn, Langmuir-Blodgett films formed by continuously varying surface pressure. Characterization by IR spectroscopy and epifluorescence microscopy, Langmuir 23 (2007) 4950–4958.
[21] K. Nag, J.S. Pao, R.R. Harbottle, F. Possmayer, N.O. Petersen, L.A. Bagatolli, Segregation of saturated chain lipids in pulmonary surfactant films and bilayers, Biophys. J. 82 (2002) 2041–2051.
[22] C. Casals, Role of surfactant protein A (SP-A)/lipid interactions for SP-A functions in the lung, Pediatr. Pathol. Mol. Med. 20 (2001) 249–268.
[23] J. Perez-Gil, Lipid-protein interactions of hydrophobic proteins SP-B and SP-C in lung surfactant assembly and dynamics, Pediatr. Pathol. Mol. Med. 20 (2001) 445–469.

[24] G.L.J. Gaines, Insoluble monolayers at liquid–gas interfaces, Wiley InterScience, New York, 1966.
[25] P. Dynarowicz-Latka, A. Dhanabalan, O.N. Oliveira Jr., Modern physicochemical research on Langmuir monolayers, Adv. Colloid Interface Sci. 91 (2001) 221–293.
[26] G. Brezesinski, H. Möhwald, Langmuir monolayers to study interactions at model membrane surfaces, Adv. Colloid Interface Sci. 100 (2003) 563–584.
[27] L.A. Bagatolli, To see or not to see: lateral organization of biological membranes and fluorescence microscopy, Biochim. Biophys. Acta 1758 (2006) 1541–1556.
[28] K. Bacia, P. Schwille, Fluorescence correlation spectroscopy, Methods Mol. Biol. 398 (2007) 73–84.
[29] R.F. de Almeida, J. Borst, A. Fedorov, M. Prieto, A.J. Visser, Complexity of lipid domains and rafts in giant unilamellar vesicles revealed by combining imaging and microscopic and macroscopic time-resolved fluorescence, Biophys. J. 93 (2007) 539–553.
[30] M. Lösche, E. Sackmann, H. Möhwald, A fluorescence microscopic study concerning the phase diagram of phospholipids, Ber. Bunsenges. Phys. Chem. 87 (1983) 848–852.
[31] I.A. Boldyrev, X. Zhai, M.M. Momsen, H.L. Brockman, R.E. Brown, J.G. Molotkovsky, New BODIPY lipid probes for fluorescence studies of membranes, J. Lipid Res. 48 (2007) 1518–1532.
[32] M. Gudmand, M. Fidorra, T. Bjornholm, T. Heimburg, Diffusion and partitioning of fluorescent lipid probes in phospholipid monolayers, Biophys. J. 96 (2009) 4598–4609.
[33] A.C. Simonsen, L.A. Bagatolli, Structure of spin-coated lipid films and domain formation in supported membranes formed by hydration, Langmuir 20 (2004) 9720–9728.
[34] U. Bernchou, J. Brewer, H.S. Midtiby, J.H. Ipsen, L.A. Bagatolli, A.C. Simonsen, Texture of lipid bilayer domains, J. Am. Chem. Soc. 131 (2009) 14130–14131.
[35] T. Parasassi, E. Kranowska, L.A. Bagatolli, E. Gratton, Laurdan and Prodan as polarity-sensitive fluorescent membrane probes, J. Fluoresc. 8 (1998) 365–373.
[36] T. Parasassi, G. De Stasio, A. d'Ubaldo, E. Gratton, Phase fluctuation in phospholipid membranes revealed by Laurdan fluorescence, Biophys. J. 57 (1990) 1179–1186.
[37] T. Parasassi, G. De Stasio, G. Ravagnan, R.M. Rusch, E. Gratton, Quantitation of lipid phases in phospholipid vesicles by the generalized polarization of Laurdan fluorescence, Biophys. J. 60 (1991) 179–189.
[38] J.B. de la Serna, G. Oradd, L.A. Bagatolli, A.C. Simonsen, D. Marsh, G. Lindblom, et al., Segregated phases in pulmonary surfactant membranes do not show coexistence of lipid populations with differentiated dynamic properties, Biophys. J. 97 (2009) 1381–1389.
[39] C. Dietrich, L.A. Bagatolli, Z.N. Volovyk, N.L. Thompson, M. Levi, K. Jacobson, et al., Lipid rafts reconstituted in model membranes, Biophys. J. 80 (2001) 1417–1428.
[40] L.A. Bagatolli, Thermotropic behavior of lipid mixtures studied at the level of single vesicles: giant unilamellar vesicles and two-photon excitation fluorescence microscopy, Methods Enzymol. 367 (2003) 233–253.
[41] L.A. Bagatolli, E. Gratton, Two-photon fluorescence microscopy observation of shape changes at the phase transition in phospholipid giant unilamellar vesicles, Biophys. J. 77 (1999) 2090–2101.
[42] L.A. Bagatolli, E. Gratton, A correlation between lipid domain shape and binary phospholipid mixture composition in free standing bilayers: a two-photon fluorescence microscopy study, Biophys. J. 79 (2000) 434–447.
[43] L.A. Bagatolli, E. Gratton, Two photon fluorescence microscopy of coexisting lipid domains in giant unilamellar vesicles of binary phospholipid mixtures, Biophys. J. 78 (2000) 290–305.
[44] J. Korlach, P. Schwille, W.W. Webb, G.W. Feigenson, Characterization of lipid bilayer phases by confocal microscopy and fluorescence correlation spectroscopy, Proc. Natl. Acad. Sci. U. S. A. 96 (1999) 8461–8466.
[45] L.A. Bagatolli, E. Gratton, G.D. Fidelio, Water dynamics in glycosphingolipid aggregates studied by LAURDAN fluorescence, Biophys. J. 75 (1998) 331–341.
[46] C.W. Hollars, R.C. Dunn, Submicron structure in L-alpha-dipalmitoylphosphatidylcholine monolayers and bilayers probed with confocal, atomic force, and near-field microscopy, Biophys. J. 75 (1998) 342–353.
[47] K.J. Klopfer, T.K. Vanderlick, Isotherms of dipalmitoylphosphatidylcholine (DPPC) monolayers: features revealed and features obscured, J. Colloid Interface Sci. 182 (1996) 220–229.
[48] P. Kruger, M. Losche, Molecular chirality and domain shapes in lipid monolayers on aqueous surfaces, Phys. Rev. E 62 (2000) 7031–7043.
[49] F. Bringezu, M. Majerowicz, S.Y. Wen, G. Reuther, K.T. Tan, J. Kuhlmann, et al., Membrane binding of a lipidated N-Ras protein studied in lipid monolayers, Eur. Biophys. J. Biophys. Lett. 36 (2007) 491–498.
[50] K. Wagner, G. Brezesinski, Modifying dipalmitoylphosphatidylcholine monolayers by n-hexadecanol and dipalmitoylglycerol, Chem. Phys. Lipids 145 (2007) 119–127.
[51] T.T. Mills, G.E.S. Toombes, S. Tristram-Nagle, D.M. Smilgies, G.W. Feigenson, J.F. Nagle, Order parameters and areas in fluid-phase oriented lipid membranes using wide angle X-ray scattering, Biophys. J. 95 (2008) 669–681.
[52] J. Pan, S. Tristram-Nagle, N. Kucerka, J.F. Nagle, Temperature dependence of structure, bending rigidity, and bilayer interactions of dioleoylphosphatidylcholine bilayers, Biophys. J. 94 (2008) 117–124.
[53] J.F. Nagle, S. Tristram-Nagle, Structure of lipid bilayers, Biochim. Biophys. Acta 1469 (2000) 159–195.
[54] A. Aroti, E. Leontidis, E. Maltseva, G. Brezesinski, Effects of Hofmeister anions on DPPC Langmuir monolayers at the air–water interface, J. Phys. Chem. B 108 (2004) 15238–15245.
[55] S. Tristram-Nagle, R. Zhang, R.M. Suter, C.R. Worthington, W.J. Sun, J.F. Nagle, Measurement of chain tilt angle in fully hydrated bilayers of gel phase lecithins, Biophys. J. 64 (1993) 1097–1109.
[56] D. Marsh, Lateral pressure in membranes, Biochim. Biophys. Acta 1286 (1996) 183–223.